Redshift and structure formation in a spatially flat inhomogeneous universe

J. W. Moffat and D. C. Tatarski
Department of Physics, University of Toronto, Toronto, Ontario, Canada M5S 1A7
(Received 12 August 1991)

We study a spherically symmetric Tolman-Bondi cosmological model with globally flat spatial sections $t=$const. We consider the model valid for the description of the Universe after matter starts to dominate. The redshift and cosmological observations in the model are examined and a simple scenario of the changes in the structure formation when compared to the standard flat Friedmann-Robertson-Walker universe is proposed. This scenario is based on the fact that in our model different parts of the Universe spend unequal periods of time in the matter-dominated era. The correction to the cold-dark-matter spatial two-point correlation function is derived. Specific cases are examined corresponding to observationally based distributions of the density. We show that this not only leads to no contradictions, but significantly improves the fit of theoretically predicted correlation functions to observations.

PACS number(s): 98.80.Dr

I. INTRODUCTION

The two founding assumptions of the Friedmann model are that the Universe is isotropic and homogeneous. However, only the isotropy can be verified directly by observations [and the recent Cosmic Background Explorer (COBE) data confirming the high degree of isotropy of the microwave background [1] seems to have done just that]. There is no fundamental physical reason for the latter of the assumptions to be rigorously correct. For obvious reasons we cannot directly probe the homogeneity of the Universe on a cosmological scale, and to justify that assumption we are left with the Copernican principle alone. Even though it is appealing since it supplies us with a mathematically simple cosmological model, referring to it as directly verifiable would be an overstatement. Quite the contrary, there seems to exist a growing body of observational evidence in favor of larger and larger structures. So far we have heard of the "great attractor" [2], the "great wall" [3], and recently about a quasar superstructure [4]. Moreover, the survey of the galaxy density field completed by Infrared Astronomy Satellite (IRAS) [5] provides indisputable evidence of an excess of large-scale clustering over that predicted by the standard cold-dark-matter (CDM) model (e.g., [6]). Attempts by some CDM protagonists to resurrect the model in a modified form require either a nonzero cosmological constant [7], or throwing massive neutrinos into the model along with CDM [8] to compensate for lack of clustering on large scales. Obviously, a complicated enough model can reproduce the observations to an acceptable accuracy, but also causes a lot of skepticism, particularly among particle physicists, who would prefer both Λ and neutrino masses to be zero.

In our opinion it is worthwhile to investigate cosmological models other than Friedmann's to examine possibilities of solving the large-scale structure problem. The second simplest model at hand (mathematically that is, conceptually, perhaps, even simpler) would be a spherically symmetrical Tolman-Bondi model [9,10]. There is no indication of such a model contradicting observations in any way, and many wide open avenues of research exist. In fact, this approach was recently used [11] to explore the possibility of a dipole moment of the microwave background as a cosmological effect rather than being caused by an infall onto the "great attractor," and also [12] in an attempt to reconcile dark-matter inhomogeneities with a homogeneous distribution of baryonic matter.

There are remarkably few restrictions imposed on the model. Obviously, the observable Universe should be smaller than the inflationary bubble it is contained in. Also the inhomogeneity should be small enough to allow at least "quasi-inflation." (Contrary to what inflation advocates want us to believe, initial spatial inhomogeneity seriously affects inflation, e.g., [13].) These restrictions apply if one treats inflation seriously. Since the inflationary scenarios change at the rate of fashion design this task is difficult. Second, the Tolman-Bondi model does not allow for pressure. This is not a serious flaw. The Universe has been matter dominated since a very early epoch, and all of the structure formation has taken place in this era. However, if we wanted to take our investigation to earlier epochs, we would probably be left only with numerical methods.

Since the Tolman-Bondi model describes an inhomogeneous universe, the most general (and natural) approach would be to impose no restrictions on the local curvature. In this manner we could study a model in which underdense parts of the universe expand forever, while others collapse in a finite time. Curvature effects would clearly influence the dynamics of the universe including structure formation. In particular, we would expect, in addition to galaxies, clusters, and superclusters, some "superstructure" on scales comparable to those of initial inhomogeneity. Such a model will be the subject of future work. In this paper we present a simpler model with globally constant curvature (for the sake of mathematical simplicity, we choose our model to be spatially flat).

In the following section we briefly describe the Tolman-Bondi model and present the spatially flat variant. Section III consists of a discussion of the redshift-distance relation and the corrections to the spatial two-point correlation function of the CDM in our model. The closing section contains a description of our results of numerical calculations as well as conclusions.

Throughout this paper we use units in which $G=c=1$, unless stated otherwise.

II. THE MODEL

First, for the sake of notational clarity, we write the Friedmann-Robertson-Walker line element

$$ds^2=dt^2-a^2(t)\left[\frac{dr^2}{1-kr^2}+r^2d\Omega^2\right], \tag{2.1}$$

with $d\Omega^2=d\theta^2+\sin^2\theta\, d\phi^2$.

Now, let us consider a Tolman-Bondi [9,10] model for a spherically symmetric inhomogeneous universe filled with dust. The line element in comoving coordinates can be written as

$$ds^2=dt^2-R'^2(t,r)f^{-2}dr^2-R^2(t,r)d\Omega^2, \tag{2.2}$$

where f is an arbitrary function of r only, and the field equations demand that $R(t,r)$ satisfies

$$2R\dot{R}^2+2R(1-f^2)=F(r), \tag{2.3}$$

with F being an arbitrary function of class C^2, $\dot{R}=\partial R/\partial t$, and $R'=\partial R/\partial r$. We have three distinct solutions depending on whether $f^2<1$, $=1$, >1 and they correspond to elliptic (closed), parabolic (flat), and hyperbolic (open) cases, respectively.

The proper density can be expressed as

$$\rho=\frac{F'}{16\pi R'R^2}, \tag{2.4}$$

and by analogy with the Friedmann model, we can define the critical density $\rho_c(t,r)$ corresponding to flat spatial sections $t=\text{const}$ ($f^2=1$):

$$8\pi\rho_c=\frac{\dot{R}^2}{R^2}+2\frac{\dot{R}}{R}\frac{\dot{R}'}{R'}. \tag{2.5}$$

In a spherically symmetric universe we have two "Hubble parameters": $H_r(t,r)$ for the local expansion rate in the radial direction and $H_\perp(t,r)$ for expansion in the perpendicular direction. Usual definitions give

$$H_r=\frac{\dot{l}_r}{l_r}=\frac{\dot{R}'}{R'}, \tag{2.6a}$$

$$H_\perp=\frac{\dot{l}_\perp}{l_\perp}=\frac{\dot{R}}{R}, \tag{2.6b}$$

where l denotes the proper distance, i.e., $l_r=R'(t,r)f^{-1}dr$ and $l_\perp=R(t,r)d\Omega$. By defining an "effective" Hubble parameter $H_{\text{eff}}^2=H_\perp^2+2H_\perp H_r$, we can rewrite (2.5) as a formal analogue of the Friedmann equation:

$$8\pi\rho_c=3H_{\text{eff}}^2.$$

We also define a local density parameter $\Omega(t,r)=\rho(t,r)/\rho_c(t,r)$. If we now solve (2.4) using (2.3) we get

$$\Omega-1=\frac{\rho}{\rho_c}-1=\frac{1}{3H_{\text{eff}}^2}\left[\frac{1-f^2}{R^2}-2\frac{f}{R}\frac{f'}{R'}\right]. \tag{2.7}$$

Because of spatial inhomogeneity this is a *local* equation for curvature in terms of density. There is a correspondence between the curvature of space and the sign of $\Omega-1$:

$\Omega-1<0$, $f^2>1$ open,

$\Omega-1=0$, $f^2=1$ flat,

$\Omega-1>0$, $f^2<1$ closed.

Whatever the curvature, the total mass of matter within comoving radius r is

$$M(r)=\tfrac{1}{4}\int_0^r dr\, f^{-1}F'=4\pi\int_0^r dr\,\rho f^{-1}R'R^2, \tag{2.8}$$

so that

$$M'(r)=\frac{dM}{dr}=4\pi\rho f^{-1}R'R^2.$$

Also for $\rho>0$ everywhere we have $F'>0$ and $R'>0$, so that in the nonsingular part of the model $R>0$ except for $r=0$ and $F(r)$ is non-negative and monotonically increasing for $r\geq 0$. This could be used to define the new radial coordinate $\bar{r}^3=M(r)$ and to find [14] the parametric solutions for the rate of expansion:

$$R=\frac{m(r)}{|2E|}[1-\cos(v)],\quad E(r)<0, \tag{2.9a}$$

$$t=\frac{m(r)}{|2E|^{3/2}}[v-\sin(v)],\quad E(r)<0, \tag{2.9b}$$

or

$$R=\frac{m(r)}{|2E|}[\cosh(v)-1],\quad E(r)>0, \tag{2.10a}$$

$$t=\frac{m(r)}{|2E|^{3/2}}[\sinh(v)-v],\quad E(r)>0, \tag{2.10b}$$

where $E(r)=\frac{1}{2}(f^2-1)$ can be interpreted as the total energy within radius r and $m(r)=\int_0^r dr\, fM'$. Clearly, (2.9) and (2.10) correspond to closed and open cases, respectively.

For simplicity we consider the globally flat case $f^2=1$ ($E=0$). The metric reduces to

$$ds^2=dt^2-R'^2dr^2-R^2d\Omega^2, \tag{2.11}$$

where

$$R=\tfrac{1}{2}(9F)^{1/3}(t+\beta)^{2/3},$$

with $\beta(r)$ an arbitrary function of r of class C^2 (we use the notation of [14]). Choosing a new radial coordinate

$$\bar{r}=\tfrac{1}{2}(9F)^{1/3}, \tag{2.12}$$

we get

$$R(t,r)=r[t+\beta(r)]^{2/3}\ , \tag{2.13}$$

where we have dropped the bar over r when adopting this choice of radial coordinate. Supposing a nonzero limit for g_{rr} as $r\to 0$, we have $R\sim r$ near $r=0$, so for finite $\dot{R}(t,0)$ we have $F(0)=0$. This requires that $\beta(r)$ has a finite limit as $r\to 0$. The metric (2.11) becomes

$$ds^2=dt^2-(t+\beta)^{4/3}(Y^2dr^2+r^2d\Omega^2)\ , \tag{2.14}$$

where

$$Y=1+\frac{2r\beta'}{3(t+\beta)}\ , \tag{2.15}$$

and from (2.4) the density is given by

$$\rho=\frac{1}{6\pi(t+\beta)^2Y}\ . \tag{2.16}$$

The model depends on one arbitrary function $\beta(r)$ and could be specified by assuming the density on some spacelike hypersurface, say $t=t_0$. In the closing section we will discuss a more observationally based method of doing that.

The metric and density are singular on the two hypersurfaces

$$t+\beta=0,\quad Y=0\ , \tag{2.17a}$$

namely,

$$t_1=-\beta,\quad t_2=-\beta-\frac{2r\beta'}{3}\ . \tag{2.17b}$$

We consider our model valid only for

$$t>\Sigma(r)\equiv\mathrm{Max}[t_1(r),t_2(r)]\ . \tag{2.18}$$

Thus, $t(r)=\Sigma(r)$ defines the big-bang hypersurface of the model. Since the model describes a universe filled with pressureless matter, we interpret it physically as the surface on which the universe enters the matter-dominated era [in the Friedmann-Robertson-Walker (FRW) model this happens everywhere at the same $t_{\rm eq}$ corresponding to $z_{\rm eq}\approx 10^4$]. It is worth noting that even in our globally flat model different parts of the universe can do that at different times.

Finally, let us notice that both the substitution $\beta=0$ and taking the limit $t\to\infty$ give the Einstein–de Sitter universe

$$ds^2=dt^2-t^{4/3}(dr^2+r^2d\Omega^2)\ . \tag{2.19}$$

This not only means that, as expected, we get the homogeneous case when $\beta=0$, but also that [14] an expanding flat Tolman-Bondi model with an everywhere nonvanishing density necessarily evolves to the homogeneous Einstein–de Sitter model, whatever the initial conditions.

III. THE REDSHIFT AND STRUCTURE FORMATION

Let us now examine the propagation of light in our model. The high degree of isotropy of the microwave background forces us to the conclusion that we must be located very close to the spatial center of the universe. In our discussion, for the sake of simplicity, we place an observer at the center ($t_{\rm ob}=t_0, r_{\rm ob}=0$).

The luminosity distance between an observer at the origin of our coordinate system $(t_0,0)$ and the source at $(t_e,r_e,\theta_e,\phi_e)$ is [10]

$$d_L=\left[\frac{\mathcal{L}}{4\pi\mathcal{F}}\right]^{1/2}=R(t_e,r_e)[1+z(t_e,r_e)]\ , \tag{3.1}$$

where $\mathcal{L}$ is the absolute luminosity of the source (the energy emitted per unit time in the source's rest frame), $\mathcal{F}$ is the measured flux (the energy per unit time per unit area as measured by the observer), and $z(t_e,r_e)$ is the redshift (blueshift) for a light ray emitted at (t_e,r_e) and observed at $(t_0,0)$.

The light ray traveling inwards to the center satisfies

$$ds^2=dt^2-R'^2(t,r)dr^2=0,\quad d\theta=d\phi=0\ ,$$

and thus

$$\frac{dt}{dr}=-R'(t,r)\ . \tag{3.2}$$

Consider two rays emitted by the source with a small time separation τ. The equation of the first ray is

$$t=T(r)\ , \tag{3.3a}$$

while the equation of the second ray is

$$t=T(r)+\tau(r)\ . \tag{3.3b}$$

Using (3.2) we get the equation of a ray and the rate of change of $\tau(r)$ along the path:

$$\frac{dT(r)}{dr}=-R'[T(r),r]\ , \tag{3.4a}$$

$$\frac{d\tau(r)}{dr}=-\tau(r)\dot{R}'[T(r),r]\ , \tag{3.4b}$$

where

$$\dot{R}'[T(r),r]=\left.\frac{\partial^2R}{\partial t\,\partial r}\right|_{r,T(r)}=\left.\frac{\partial R'}{\partial t}\right|_{r,T(r)}\ .$$

If we take $\tau(r_e)$ to be the period of some spectral line at r_e then

$$\frac{\tau(0)}{\tau(r_e)}=\frac{\nu(r_e)}{\nu(0)}=1+z(r_e),\quad z=0\ \text{ for } r_e=0\ .$$

The equation for the redshift considered as a function of r along the light cone is

$$\frac{dz}{dr}=(1+z)\dot{R}'[T(r),r]\ , \tag{3.5}$$

where $T(r)$ is given by (3.4a). The shift z_1 for a light ray traveling from (t_1,r_1) to $(t_0,0)$ is

$$\ln(1+z_1)=-\int_0^{r_1}dr\,\dot{R}'[T(r),r]\ . \tag{3.6}$$

To see how this differs from the Friedmann-Robertson-Walker case we assume (in a manner similar to that of [10]) that R is an increasing function of r and relabel the radial coordinate $\bar{r}=R[T(r),r]$. Also,

$$a_1(r)=\dot{R}[T(r),r],\quad a_2(r)=\ddot{R}[T(r),r],\ldots,$$

are functions of r only. Expanding (3.6) and keeping terms to linear order we get

$$\ln(1+z_1)=\int_0^{r_1}dr\frac{a_1'}{1-a_1}-\int_0^{r_1}dr\frac{a_1a_1'-a_2}{1-a_1}$$
$$=-\ln(1-a_1)-\int_0^{r_1}dr\frac{M'(r)}{r(1-a_1)}\ , \qquad (3.7)$$

where, in obtaining the second equation, we used (2.4) and (2.8). Thus we have two contributions to the redshift: the cosmological redshift due to expansion, described by the first term with $a_1=\dot{R}$, and the shift due to the difference between the potential energy per unit mass at the source and at the observer. Obviously, in the homogeneous case $[M'(r)=0]$ there is no gravitational shift.

To complete the discussion let us notice that the integral in (3.7) can be rewritten as

$$\int_0^{r_1}dr\frac{4\pi\rho r}{(1-a_1)^2}\ ,$$

and for small r_1 can be neglected when compared to the first term. Expanding the logarithms on both sides of (3.7) we see that light emitted at (t_e,r_e) and observed at $(t_0,0)$ satisfies for small r_e or small t_0-t_e:

$$z(t_e,r_e)=\dot{R}(t_e,r_e)\ ,$$

where t_e is $T(r_e)$ from (3.4a) with the initial condition $T(0)=t_0$. Using (2.6b) and (3.1) we get, for small r_e,

$$z(t_e,r_e)=H_\perp(t_e,r_e)d_L(t_e,r_e)\ , \qquad (3.8)$$

which is formally analogous to the FRW result. Two main differences are that our relation is *local* and that from cosmological observations we obtain the angular Hubble parameter $H_\perp=\dot{R}/R$ rather than FRW's $H_F=\dot{a}/a$.

Let us now turn our attention to the structure formation. We do not postulate any major departures from the mechanisms considered in FRW (for an overview see, e.g., [15]). However, we comment on the possibility of such a divergence in the closing section. Since a "standard model" of structure formation in a homogeneous universe still does not exist, we concentrate on the CDM mechanism [6], which not long ago seemed to provide a satisfactory picture but recently found itself in difficulty. We assume that the primary difference between CDM scenarios of structure formation in a FRW model and in our inhomogeneous flat model is the amount of time different parts of the universe have spent in the matter-dominated era.

The main assumptions of the CDM mechanism are that the Universe is flat and dominated by weakly interacting massive particles (WIMP's). It enters the matter-dominated era with scale-invariant, Gaussian, and adiabatic initial fluctuations generated in the early epochs. These primeval inhomogeneities started growing after decoupling via gravitational instability to form the structure we see today.

The standard apparatus used to describe the density field of the Universe in the spatially flat models includes the density contrast

$$\delta(\mathbf{x})\equiv\frac{\delta\rho(\mathbf{x})}{\bar{\rho}}=\frac{\rho(\mathbf{x})-\bar{\rho}}{\bar{\rho}} \qquad (3.9)$$

and its Fourier expansion

$$\delta_k=V^{-1}\int_{\rm vol}d^3x\ \delta(\mathbf{x})\exp(i\mathbf{k}\cdot\mathbf{x})\ , \qquad (3.10)$$

where $\bar{\rho}$ is the average density of the Universe [in the spherically symmetric case it may be convenient to use $\delta(r)=\delta(\mathbf{r})$]. For Gaussian random fluctuations statistical quantities may be specified in terms of the power spectrum $|\delta_k|^2$. If one considers the rms density fluctuations

$$\frac{\delta\rho}{\rho}=\langle\delta(\mathbf{x})\delta(\mathbf{x})\rangle^{1/2}\ ,$$

where the angular brackets denote averaging over all space, it follows that, for an isotropic power spectrum (i.e., depending on $k=|\mathbf{k}|$ rather than $\mathbf{k}$),

$$\left[\frac{\delta\rho}{\rho}\right]^2=V^{-1}\int_0^\infty\frac{k^3|\delta_k|^2}{2\pi^2}\frac{dk}{k}\ , \qquad (3.11)$$

where the quantity $(k^{3/2}|\delta_k|)/(\sqrt{2}\pi)$ describes the contribution to $\delta\rho/\rho$ from a given logarithmic interval in k and is often referred to as the processed power spectrum.

Finally, if we define the mass autocorrelation function $\xi(\mathbf{r})$,

$$\xi(\mathbf{r})\equiv\langle\delta(\mathbf{x}+\mathbf{r})\delta(\mathbf{x})\rangle\ , \qquad (3.12)$$

one can verify that it is the Fourier transform of the power spectrum:

$$\xi(\mathbf{r})=\frac{1}{(2\pi)^3V}\int d^3k|\delta_k|^2\exp(-i\mathbf{k}\cdot\mathbf{r})\ , \qquad (3.13a)$$

$$|\delta_k|^2=V\int d^3r\ \xi(\mathbf{r})\exp(i\mathbf{k}\cdot\mathbf{r})\ . \qquad (3.13b)$$

In our isotropic case $\xi(\mathbf{r})=\xi(r)$. It also follows that $\xi(0)=(\delta\rho/\rho)^2$.

In the standard version of the CDM model the power spectrum (if baryons contribute a small fraction of the density, i.e., $\Omega_B\ll\Omega_0$) is given by [16]

$$|\delta_k|^2=\text{const}\times k/\{1+[ak+(bk)^{3/2}+(ck)^2]^\nu\}^{2/\nu}\ , \qquad (3.14)$$

where $a=6.4(\Omega_0h^2)^{-1}$ Mpc, $b=3.0(\Omega_0h^2)^{-1}$ Mpc, $c=1.7(\Omega_0h^2)^{-1}$ Mpc, $\nu=1.13$, and h is the FRW Hubble parameter in units of 100 km s^{-1} Mpc^{-1}. The spatial two-point correlation function obtained from (3.14) using (3.13) and the power law $\xi_{\rm GG}(r)\simeq(r/5.5\ \text{Mpc})^{-1.7}$, corresponding to the galaxy-galaxy correlation function at galaxy separations $0.1h^{-1}\ \text{Mpc}\le r\le 20h^{-1}\ \text{Mpc}$, will be shown parallel to our results in the figures of the next section. Since the cluster-cluster correlation function is [15] $\xi_{\rm CC}(r)\simeq(r/25\ \text{Mpc})^{-1.7}$, it is clear that $\xi(r)$ as predicted by CDM falls well below the data both on small and large scales. As mentioned earlier, attempts to cure this problem require "exotic" physics and even then do not lead to

the solution on scales $\geq 10h^{-1}$ Mpc.

Leaving aside subtleties of the time evolution of density inhomogeneities in a FRW model, let us recall [15] its main features. For both subhorizon and superhorizon perturbations there are two physical modes: a growing mode and a decaying one. Subhorizon perturbations do not grow during the radiation-dominated era, while the growing mode of the superhorizon perturbations evolves as $(\delta\rho/\rho)_+ \equiv \delta_+ \propto t$. During the matter-dominated era both growing modes evolve as $\delta_+ \propto t^{2/3}$. Hence, it seems reasonable (since in Tolman-Bondi models we are confined to the matter-dominated era) to assume in the first approximation that in our inhomogeneous flat model density perturbations also grow as $\delta \propto t^{2/3}$ independently of their scales. We also assume that entering the matter-dominated era [i.e., at the time $t(r)=\Sigma(r)$ given by the big-bang hypersurface of our model] our Universe had the spectrum of primeval fluctuations identical to that of the CDM FRW model at the corresponding epoch $t_{\rm eq}$ [even though formally the density on $\Sigma(r)$ is infinite].

In FRW we have, for the growing mode,

$$\delta_F(t)=\delta_F(t_{\rm eq})\left[\frac{t_F}{t_{\rm eq}}\right]^{2/3}, \tag{3.15}$$

where we normalized the solution at $t_{\rm eq}$ and t_F denotes the (same everywhere in space) time from the initial singularity in the FRW model to a given value of time coordinate t.

In our inhomogeneous isotropic flat model we have

$$\delta_T(t,r)=\delta_T(t_\Sigma(r),r)\left[\frac{t_T(r)}{t_\Sigma(r)}\right]^{2/3}, \tag{3.16}$$

where again $t_T(r)=t-\Sigma(r)$ is the time from the initial singularity (2.18) of our model to a given value of time coordinate t. Also, by our simplifying assumptions,

$$\delta_F(t_{\rm eq})=\delta_T(t_\Sigma(r),r) \quad \text{and} \quad t_{\rm eq}=t_\Sigma(r) \quad \text{for all } r .$$

Thus for some value of time coordinate t,

$$\delta_T(t,r)=\left[\frac{t_T(r)}{t_F}\right]^{2/3}\delta_F(t), \tag{3.17}$$

which clearly shows that on some spacelike hypersurface $t=\text{const}$, the extent of the gravitational amplification of small primeval perturbations depends on position. The larger $t_T(r)$ for a given r, the more developed structure we expect to see there.

In our isotropic model we ("the observers") are located at $(t_0,0)$; thus we can write the spatial two-point correlation function as

$$\xi_T(t_0,r)=\langle \delta_T(t_0,r)\delta_T(t_0,0)\rangle . \tag{3.18}$$

Using (3.17) and the fact that $t_T(0)=t_F$, we finally arrive at the correction to the FRW correlation function $\xi_F(r)$ in (3.12) as given by our model:

$$\xi_T(r)=\left[\frac{t_T(r)}{t_F}\right]^{2/3}\xi_F(r) . \tag{3.19}$$

IV. RESULTS AND DISCUSSION

We first rewrite the basic formulas in the language of the metric (2.14), i.e., using $\beta(r)$. The Hubble parameters (2.6) become

$$H_r=\frac{\dot R'}{R'}=\frac{2}{3}(t+\beta)^{-1}\frac{3(t+\beta)-r\beta'}{3(t+\beta)+2r\beta'} , \tag{4.1a}$$

$$H_\perp=\frac{\dot R}{R}=\frac{2}{3}(t+\beta)^{-1} . \tag{4.1b}$$

Let us denote the observationally determined value of the Hubble constant as $H_0=100h$ km s^{-1} Mpc^{-1}. The reported values of h span the range (0.4;1).

In the FRW model $H_0=H_F(t_0)=(\dot a/a)_{t_0}$ sets the age of the matter-dominated universe at

$$t_F=t_0=\frac{1}{H_0}\int_0^1 dx(1-\Omega_0+\Omega_0/x)^{-1/2} .$$

For the flat FRW case ($\Omega_0=1$),

$$t_F=t_0=\frac{2}{3H_0} . \tag{4.2}$$

The big-bang singularity is at $t=0$.

Our discussion in the previous section showed that if we were to interpret the cosmological tests (such as the redshift-luminosity one) in the spirit of our inhomogeneous model, we would have to assign H_0 to $H_\perp(t_0,0)$. To be more precise this would be the case for H_0 derived from observations at small redshifts.

At $r=0$ the big-bang hypersurface of our model is located at $\Sigma(0)=-\beta(0)$, since the requirement that $\beta(r)$ have a finite limit as $r\to 0$ forces $\beta'(0)=0$. Thus for the observer at $(t_0,0)$, where t_0 is the time coordinate of constant time hypersurface "now," the age of the Universe is determined by

$$t_T(0)=t_0+\beta(0)=\frac{2}{3H_\perp(t_0,0)}=\frac{2}{3H_0} . \tag{4.3}$$

This, when compared to (4.2), sets $\beta(0)=0$ and $t_F=t_T(0)$. Consequently, we must have

$$\rho_T(t_0,0)=\rho_{cF}(t_0)=\frac{3H_0^2}{8\pi} .$$

We see that our model does not solve the so-called "age of the Universe" problem (e.g., [15]), at least not at its spatial center. We cannot claim that at $r=0$ our Universe had sufficiently more time since the big bang to accommodate uncomfortable estimates of the age of globular clusters, the age of the Galaxy based on radioactive dating, etc. In fact, at the center it has existed for exactly the same time as a matter-dominated flat FRW universe. However, in principle, we could solve the problem for outer parts of the Universe by choosing $\beta(r)$ so that $\Sigma(r)$ decreases with r. In this manner we would have a universe in which the outer parts were older and the center youngest. Obviously, there remains the ultimate question of whether such a model would be consistent with observations.

Let us now write the system of equations we work with

in a form suitable for numerical calculations. Equations (3.4) can be written as

$$\frac{dT(r)}{dr}=-[T(r)+\beta(r)]^{2/3}\left[1+\frac{2r\beta'(r)}{3[T(r)+\beta(r)]}\right], \tag{4.4a}$$

$$\frac{d\tau(r)}{dr}=-\frac{2}{3}\tau(r)[T(r)+\beta(r)]^{-1/3}\left[1-\frac{r\beta'(r)}{3[T(r)+\beta(r)]}\right], \tag{4.4b}$$

with initial conditions $T(0)=t_0,\tau(0)=1$. Also,

$$z(r)=\frac{\tau(0)}{\tau(r)}-1=\frac{1}{\tau(r)}-1 . \tag{4.5}$$

For numerical calculations we choose units with $t_0=1$.

We need to supplement system (4.4) with another equation specifying $\beta(r)$. As mentioned before, we can do it by assuming the density distribution on a certain spacelike hypersurface $t=t_d$. The density of our flat model is defined by (2.4) and ($t_d=t_0$) is given "now" by

$$\rho(t_0,r)=\frac{1}{6\pi}[t_0+\beta(r)]^{-2}\left[1+\frac{2r\beta'(r)}{3[t_0+\beta(r)]}\right]^{-1}, \tag{4.6}$$

which could close our system of equations. However, this approach requires from us instantaneous, "absolute" knowledge of the density distribution throughout the Universe—rather a God-like feature. We prefer another method, directly coupled to observations.

One of the most challenging tasks in observational cosmology is measuring the mass density of the Universe. The results are usually quoted in terms of the FRW density parameter $\Omega_0=(\rho/\rho_c)_0$ and obtained either by kinematical or dynamical methods. Kinematic tests (such as the redshift-luminosity or the redshift-galaxy number count) used to determine Ω_0 are biased by their interpretations within a specific (i.e., FRW) cosmological model. Dynamical methods are to a certain extent free of this bias. The simplest are based on the use of Kepler's third law to detect the gravitational effect of the mass distribution within a galaxy on its components. The method can be extended to determine the average mass per galaxy in a cluster or that of a cluster in a supercluster. This is achieved by assuming that the system is gravitationally bound and well relaxed and then applying the viral theorem to it. The dependence on the cosmological model comes into play only through assigning the distances from the observer to the dynamical system under consideration.

All cosmological observations are necessarily done by detecting some form of electromagnetic radiation. Thus, it seems reasonable to assume that whatever mapping of the density parameter they provide, it actually describes the density along the light cone. Thus, we can specify $\beta(r)$ by closing the system (4.4) with an observationally based equation

$$\rho[T(r),r]=\frac{1}{6\pi}[T(r)+\beta(r)]^{2}\left[1+\frac{2r\beta'(r)}{3[T(r)+\beta(r)]}\right]^{-1} . \tag{4.7}$$

Since the standard notation utilizes Ω_0, it is convenient to rewrite the last two equations using the ratio of the local density in our model to the critical density of the FRW universe. Let us call it the density ratio and denote

$$\mathcal{Q}(t,r)=\frac{\rho_T(t,r)}{\rho_{cF}(t)}=\frac{t^2}{[t+\beta(r)]^2}\left[1+\frac{2r\beta'(r)}{3[t+\beta(r)]}\right]^{-1} .$$

Thus, having the form of the density ratio either for a spacelike hypersurface ($t=t_0$) $\mathcal{Q}_0(r)$ or along the light cone $\mathcal{Q}_{\rm LC}(r)$, we close the system (4.4) with one of the equations

$$\mathcal{Q}_0(r)=\frac{t_0^2}{[t_0+\beta(r)]^2}\left[1+\frac{2r\beta'(r)}{3[t_0+\beta(r)]}\right]^{-1}, \tag{4.8a}$$

$$\mathcal{Q}_{\rm LC}(r)=\frac{T^2(r)}{[T(r)+\beta(r)]^2}\left[1+\frac{2r\beta'(r)}{3[T(r)+\beta(r)]}\right]^{-1} . \tag{4.8b}$$

We are now ready to investigate particular cases in our model specified by the choice of the density ratio [giving the so far arbitrary function $\beta(r)$]. With our system of equations closed by this choice, we solve for $\beta(r)$, $T(r)$, and $\tau(r)$ and use (4.5) to obtain $z(r)$; consequently, $z(t)$ is obtained as the parametric relation $[T(r),z(r)]$. Next, we find the initial singularity hypersurface $\Sigma(r)$ of the model with the help of (2.18). Utilizing (3.19) then gives the corrected two-point spatial correlation function in our model.

First, let us demonstrate how the properties of the model are affected by the choice of either (4.8a) or (4.8b) as the equation closing the system.

The absence of quasars at large z prompted the suggestion that there is a genuine absence of visible matter at large spatial distances [17], thus, forcing the conclusion that the visible Universe is a baryon island surrounded by dark matter or even a vacuum. This proposal, however, is concerned with scales so large (corresponding to $z\gtrsim 5$) that other explanations exist, such as selection effects of observations or evolutionary corrections. We do not argue in favor of either of the above interpretations, but simply use the inferred density distribution to present the properties of the model.

Let us assume that the density ratio on the "now" hypersurface $\mathcal{Q}_0(r)$, (4.8a), has the Gaussian form of Fig. 1(a). (Here, as in all figures, the distance r is in Mpc.) This would not be the directly observed spatial distribution of the density parameter. The solution for $\beta(r)$ in this case [Fig. 1(b)] is monotonically increasing and $\Sigma(r)=-\beta(r)$. This corresponds to the already mentioned universe in which the outer parts are older and the center youngest. We have $t_T(r)\geq 10t_0$ for $r\geq 1000$ Mpc. However, inspection of Fig. 1(c) excludes this case (at least for the scale and depth of inhomogeneity assumed here) as observationally viable. The FRW redshift-time relation z_F (plotted in the same figure for reference) easily accommodates observations, while the maximum of z_T is an or-

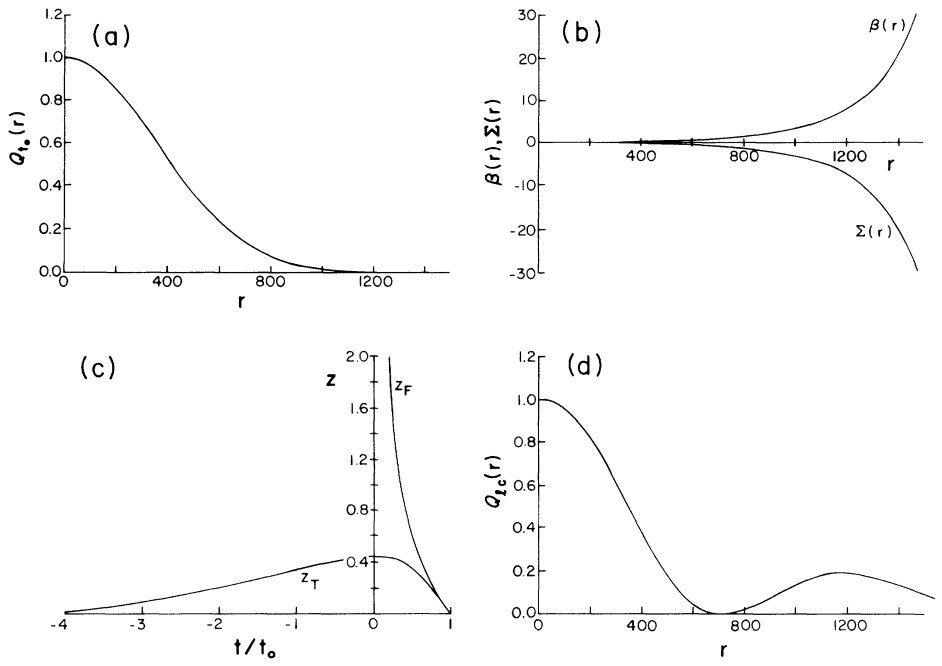

FIG. 1. (a) The density ratio on the hypersurface $t=t_0$, $\mathcal{Q}_0(r)=\exp[-(r/r_1)^2]$ with $r_1=500$ Mpc. (b) The solutions for $\beta(r)$ and $\Sigma(r)$ with $\mathcal{Q}_0(r)$ as in Fig. 1(a) [$\beta(r)$ and $\Sigma(r)$ in units of t_0]. (c) The redshift-time relation z_T in the model with $\beta(r)$ as in Fig. 1(b). The FRW relation z_F is also plotted. (d) The observed density ratio (along the light cone) $\mathcal{Q}_{\rm LC}(r)$ in the model with $\beta(r)$ as in Fig. 1(b).

der of magnitude smaller than the largest actually observed redshifts. The physical reason for the redshift to decrease with distance (large and negative times) after reaching the maximum comes from the gravitational blueshift due to the centered mass distribution that more than compensates for the redshift engendered by the expansion. Finally, Fig. 1(d) shows $\mathcal{Q}_{\rm LC}(r)$, i.e., the observationally obtainable density ratio distribution for this case. This distribution has an unexpected feature, namely, that despite the exponentially decreasing density on the hypersurface of constant time, there is a maximum in the observable density ratio $\mathcal{Q}_{\rm LC}(r)$ following the "void" at $r\gtrsim r_1=500$ Mpc (where $\mathcal{Q}_0(r)\sim\exp[-(r/r_1)^2]$) from which the distribution again tends to zero as $r\to\infty$.

Now we reinterpret the postulate of [17] by assuming that the exponential decrease in the density ratio with distance is the observed effect. The corresponding $\mathcal{Q}_{\rm LC}(r)$ is shown in Fig. 2(a) and is identical to the $\mathcal{Q}_0(r)$ of Fig. 1(a). We use this to show that superficial similarities in the two types of density ratios do not lead to analogous solutions. In fact, $\beta(r)$ as seen in Fig. 2(b) is no longer a monotonically increasing function of r and, consequently, the big-bang hypersurface of the model $\Sigma(r)\neq-\beta(r)$. The initial singularity surface is well approximated by the FRW singularity $t=0$ for $r\gtrsim 1500$ Mpc. Moreover, the time scales involved are substantially reduced: $\max[t_T(r)]\simeq 1.4t_0$ for $r\simeq 900$ Mpc. As intuitively expected from the form of $\Sigma(r)$, the density distribution [shown in Fig. 2(d)] tends to the homogeneous FRW limit as $r\to\infty$. The redshift-time relation z_T displayed in Fig. 2(c) cannot be as easily rejected on observational grounds as the one from the previous case. Nevertheless, it has some features which are difficult to explain. Even though it has the "correct" asymptotic behavior ($z\to\infty$ for $t\to 0$), its time dependence differs substantially from that of z_F for $z\gtrsim 0.25$. This would lead to considerable changes in our understanding of the "standard candles" in the Universe, particularly as to evolutionary corrections. For example, all objects with moderately large redshifts, say 0.25 to 1 (this, in the case under consideration, corresponds to distances of ~ 500 to ~ 1000 Mpc), would have significantly more time from the big bang to the moment when they emitted light which we now see. On the contrary, objects with large redshifts, say $z>2$ (or $r>1500$ Mpc) would have much less time to evolve before emitting their light. This can be regarded as a drawback: too little time for quasars to sufficiently evolve, or an advantage: an explanation of why we see so relatively few objects with large redshifts. Since we treat the particular forms of the density ratios here only as means to probe the properties of the model, we leave the choice to the reader. This exercise can serve as a probe of one's universal optimism (or pessimism).

In neither of the above cases do we achieve a significant success in correcting the FRW CDM two-point correlation function using (3.19). In the first case, this results from the fact that considerable growth in the correction factor $[t_T(r)/t_F]^{2/3}$ takes place for distances much larger than 100 Mpc, thus leaving $\xi(r)$ unchanged for the scales $1\lesssim r\lesssim 100$ Mpc, where we seek improve-

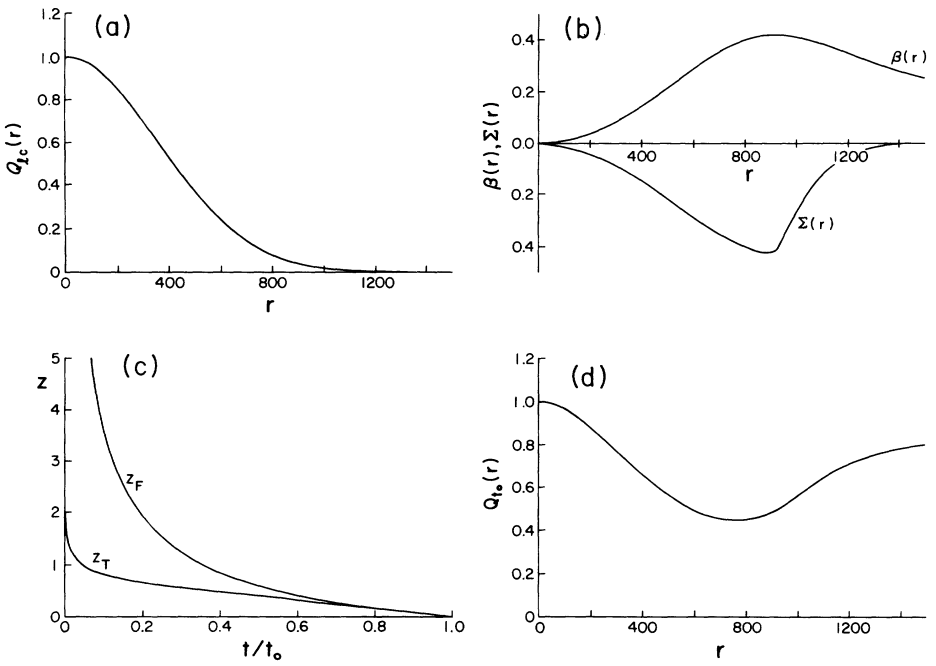

FIG. 2. (a) The density ratio along the light cone $\mathcal{Q}_{LC}(r)=\exp[-(r/r_1)^2]$ with $r_1=500$ Mpc. (b) The solutions for $\beta(r)$ and $\Sigma(r)$ with $\mathcal{Q}_{LC}(r)$ as in Fig. 2(a) [$\beta(r)$ and $\Sigma(r)$ in units of t_0]. (c) The redshift-time relation z_T in the model with $\beta(r)$ as in Fig. 2(b). The FRW relation z_F is also plotted. (d) The density ratio on the hypersurface $t=t_0$, $\mathcal{Q}_0(r)$ in the model with $\beta(r)$ as in Fig. 2(b).

ment. The same is true in the second case, where also the maximum correction factor is small (for $r\simeq 900$ Mpc we have $[t_T(r)/t_F]^{2/3}\simeq(1.4)^{2/3}\simeq 1.25$).

From now on we restrict ourselves to spatial scales that have been well probed observationally, i.e., up to a few hundred Mpc. On such scales the most striking feature of the luminous matter distribution is the existence of large voids surrounded by sheetlike structures containing galaxies (e.g., [3]). The surveys [3,5] give a typical size of the voids of the order 50–$60h^{-1}$ Mpc. There has also been some evidence [18], with less certainty, for the existence of larger underdense regions with characteristic sizes of about $130h^{-1}$ Mpc. At the same time dynamical estimates of the FRW density parameter Ω_0 give very different results on different scales. The observations of galactic halos on scales less than about 10–30 Mpc typically give (see, e.g., [19]) $\Omega_{10-30}\simeq 0.2\pm 0.1$. On the other hand, smoothing the observations over larger scales (>20 Mpc, say ~ 100 Mpc) indicates (e.g., [5]) the existence of a less clustered component with a contribution exceeding 0.2, and perhaps as high as $\Omega_{\sim 100}\simeq 0.8\pm 0.2$.

We choose to interpret these observations as a confirmation that we may live in a relatively large underdense region. Obviously, our model limits us to the assumption of a spherically symmetric void. Further, since the flat model we use here necessarily restricts the local (central) density to that of the FRW critical density $\rho_T(t_0,0)=\rho_{cF}(t_0)$, we have to assume that the void surrounds the central peak. (This assumption can be avoided in the generalization to the nonflat case $f^2\neq 1$.) In our calculations we approximate the observable density ratio $\mathcal{Q}_{LC}(r)$ with

$$\mathcal{Q}_{LC}(r)=a_0+(1-a_0)\exp\left[-\left[\frac{r}{r_0}\right]^2\right]+(a_1-a_0)\left[1-\left[\frac{r}{r_1}\right]^2\frac{\exp(r/r_1)}{[\exp(r/r_1)-1]^2}\right], \tag{4.9}$$

where a_0 regulates the minimum value of $\mathcal{Q}_{LC}(r)$, a_1 is its asymptotic value for $r\to\infty$, r_0 sets the distance from the center to the point where the minimum occurs, and r_1 governs the distance at which the density ratio starts approaching its asymptotic value a_1. The $\mathcal{Q}_{LC}(r)$ satisfactorily corresponds to the physical assumptions we made. In our computations we varied a_0 in the range (0;0.1), $a_1\in(0.8;0.9)$, $r_0\in(10;20)$ Mpc, and $r_1\in(20;100)$ Mpc.

We present four sample density ratio distributions in Figs. 3(a)–3(d). In the following figures the results corresponding to a given observed density will be allocated the same letter. Figure 4 displays the solutions for $\beta(r)$ and $\Sigma(r)$ for the density ratios given in Fig. 3. The properties of the solutions are as intuitively anticipated. The age of the Universe at any given point is set by the density. The less dense the region the longer the time since the initial singularity. We note that the solutions confirm the guess that the age of the Universe should asymptotically tend to some limit $t_\infty<t_0$ as $r\to\infty$, since the density ratio (4.9) at infinity has a limit smaller than the central value. Also, the spatial extent of the older regions is correlated with the boundaries of the underdense parts of $\mathcal{Q}_{LC}(r)$. The minima in $\Sigma(r)$ are $\simeq -1.9t_0$ for $r\simeq 25$ Mpc in case (a), $\simeq -7.1t_0$ for $r\simeq 33$ Mpc in case (b), $\simeq -1.14t_0$ for $r\simeq 25$ Mpc in case (c), and $\simeq -1.1t_0$ for $r\simeq 40$ Mpc in

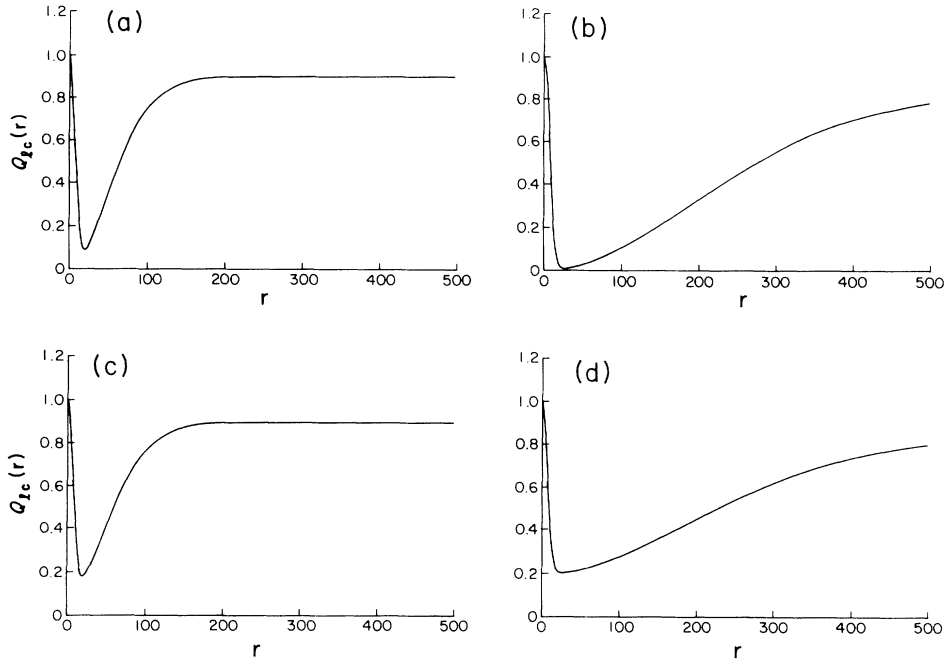

FIG. 3. The density ratios along the light cone $Q_{LC}(r)$ as given by (4.9) with (a) $r_0=10$ Mpc, $r_1=20$ Mpc, $A_0=0$, and $a_1=0.9$; (b) $r_0=10$ Mpc, $r_1=80$ Mpc, $a_0=0$, and $a_1=0.85$; (c) $r_0=10$ Mpc, $r_1=20$ Mpc, $a_0=0.1$, and $a_1=0.9$; (d) $r_0=10$ Mpc, $r_1=80$ Mpc, $a_0=0.2$, and $a_1=0.85$.

case (d). Thus, we expect noticeable corrections in $\xi(r)$ for scales $\gtrsim 10$ Mpc.

In Fig. 5 we present the redshift-time relations for the assumed distributions. There is no dramatic departure from the FRW relation. This is a positive result, since it makes the model observationally indistinguishable from the standard redshift-distance predictions.

Figure 6 contains our main results, namely, the corrected two-point spatial correlation functions $\xi_T(r)$ for the voidlike density distributions considered. Also plotted is the FRW CDM spatial two-point correlation function obtained from (3.14) using (3.13) and the "observed" power law $\xi(r)\simeq(r/5.5\ \text{Mpc})^{-1.7}$.

We think that these results are promising. There are significant excesses in the corrected two-point correlation functions $\xi_T(r)$ over the $\xi_F(r)$ on the scales from the very

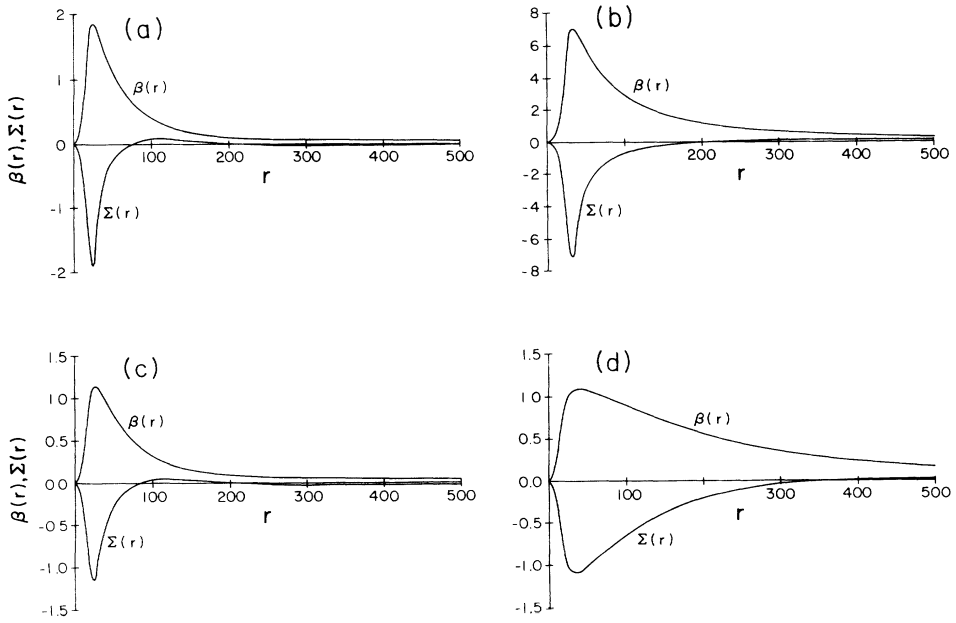

FIG. 4. The solutions for $\beta(r)$ and $\Sigma(r)$ [$\beta(r)$ and $\Sigma(r)$ in units of t_0]: (a) for $Q_{LC}(r)$ as in Fig. 3(a), (b) for $Q_{LC}(r)$ as in Fig. 3(b), (c) for $Q_{LC}(r)$ as in Fig. 3(c), (d) for $Q_{LC}(r)$ as in Fig. 3(d).

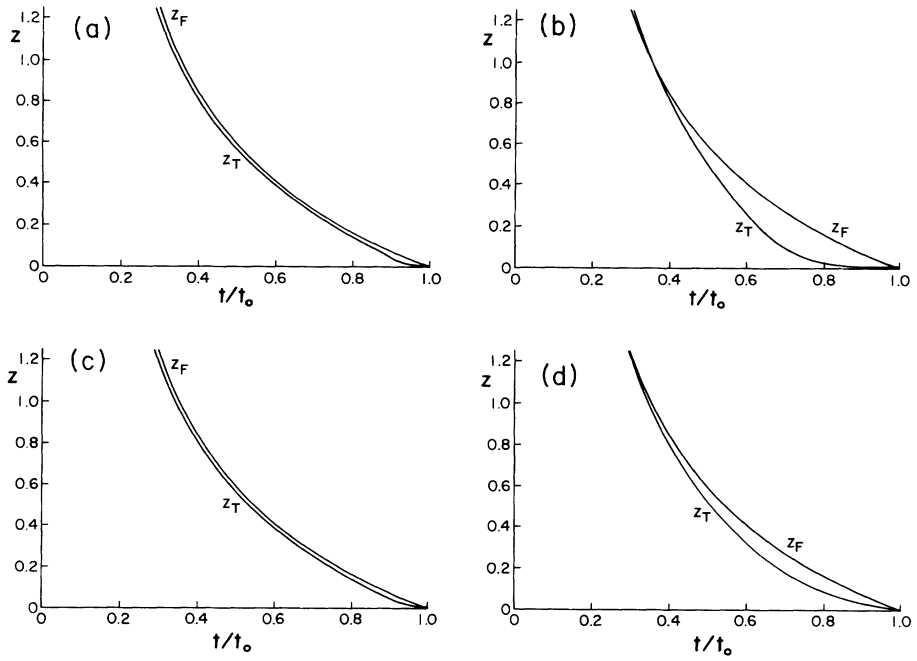

FIG. 5. The redshift-time relations z_T in the Tolman-Bondi model. The FRW relations z_F are also plotted: (a) for $\beta(r)$ as in Fig. 4(a), (b) for $\beta(r)$ as in Fig. 4(b), (c) for $\beta(r)$ as in Fig. 4(c), (d) for $\beta(r)$ as in Fig. 4(d).

small to the comparable to the outer sizes of the voids. The excess in each case is more evident on larger scales. There is an apparent improvement in the range, say, from 1 to ~ 100 Mpc. Our results do not exactly fit the observed $\xi(r) \propto (r/r_0)^{-1.7}$. However, one has to remember that we employed an *ad hoc* density ratio designed to correspond roughly to general features of the observational picture. Moreover, the galaxy-galaxy and cluster-cluster correlation functions have only approximately the same power law and much different correlation length r_0 [$25h^{-1}$ Mpc for $\xi_{CC}(r)$ compared to $5h^{-1}$ Mpc for $\xi_{GG}(r)$], so that the importance of the exact fit to the observed $\xi(r)$ should not be exaggerated.

The method we employed has certain drawbacks. The dominant one is the flatness of the model, which forbids us from considering a true void (i.e., one without a cen-

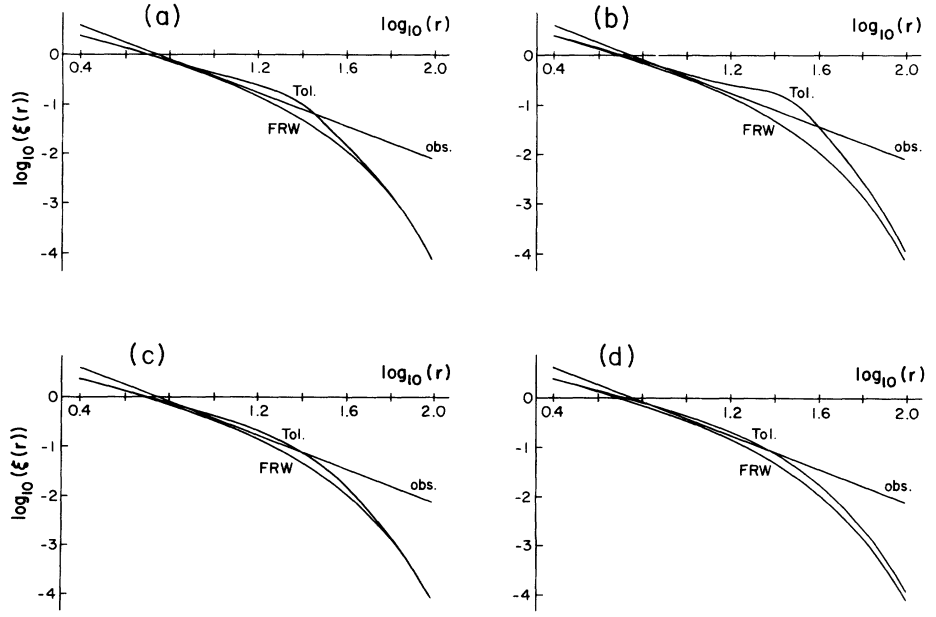

FIG. 6. The spatial two-point correlation functions [$\xi_F(r)$ is denoted by "FRW" and $\xi_T(r)$ by "Tol."; the power law $\xi(r)=(r/5.5\ \text{Mpc})^{-1.7}$ is shown as "obs."] (a) corresponding to the model with the density profile 3(a), (b) corresponding to the model with the density profile 3(b), (c) corresponding to the model with the density profile 3(c), (d) corresponding to the model with the density profile 3(d).

tral peak in the density). It also forces us to assume that the time spent in the matter-dominated era is the only significant difference between the structure formation mechanisms in FRW and our model. This is connected to the choice of CDM scenario, which requires the flat model. We chose CDM despite its difficulties, because it is the most successful model of structure formation. However, if the recent trend in the measurements of the microwave background continues, and the limits on its anisotropy go even lower, the CDM model may find itself in serious difficulty (e.g., [20]).

The above-mentioned problems can be cured by giving up the flatness of the model. This would introduce technical difficulties, but at the same time would make the model much richer. The Universe at the beginning would be very similar to the FRW model, but very different at late stages. The initial similarity would make it much more natural to use methods and ideas of the FRW cosmology to describe the primeval fluctuations. At the same time, the evolution leading to creation of underdense parts of the Universe enveloped by overdense parts could explain the surfacelike structure of galaxies surrounding voids. This type of model is the natural continuation of the present work.

ACKNOWLEDGMENTS

The authors thank N. Kaiser and J. R. Bond for discussions. This work was supported by the Natural Sciences and Engineering Research Council of Canada. One of the authors (D.C.T.) thanks the Ministry of Colleges and Universities of the Province of Ontario for financial support.

[1] J. C. Mather *et al.*, Astrophys. J. Lett. **354**, L37 (1990); C. J. Hogan, Nature (London) **344**, 107 (1990).
[2] D. Lynden-Bell *et al.*, Astrophys. J. **326**, 19 (1988).
[3] M. J. Geller and J. P. Huchra, Science **246**, 897 (1989).
[4] R. G. Clowes and L. E. Campusano, Mon. Not. R. Astron. Soc. **249**, 218 (1991).
[5] G. Efstathiou *et al.*, Mon. Not. R. Astron. Soc. **247**, 10 (1990); W. Saunders *et al.*, Nature (London) **349**, 32 (1991).
[6] M. Davis *et al.*, Astrophys. J. **292**, 371 (1985); S. D. White *et al.*, *ibid.* **313**, 505 (1987); C. S. Frenk *et al.*, *ibid.* **351**, 10 (1980).
[7] G. Efstathiou, W. J. Sutherland, and S. J. Maddox, Nature (London) **348**, 705 (1990).
[8] D. W. Sciama, Nature (London) **348**, 617 (1990).
[9] R. C. Tolman, Proc. Natl. Acad. Sci. U.S.A. **20**, 169 (1934).
[10] H. Bondi, Mon. Not. R. Astron. Soc. **107**, 410 (1947).
[11] B. Paczynski and T. Piran, Astrophys. J. **364**, 341 (1990).
[12] J. W. Moffat, University of Toronto Report No. UTPT-91-05, 1991 (unpublished).
[13] D. S. Goldwirth and T. Piran, Phys. Rev. D **40**, 3263 (1989); Phys. Rev. Lett. **64**, 2852 (1990).
[14] W. B. Bonnor, Mon. Not. R. Astron. Soc. **159**, 261 (1972); **167**, 55 (1974).
[15] P. J. E. Peebles, *The Large-Scale Structure of the Universe* (Princeton University Press, Princeton, NJ, 1980); E. W. Kolb and M. S. Turner, *The Early Universe* (Addison-Wesley, Redwood City, CA, 1990).
[16] J. R. Bond and G. Efstathiou, Astrophys. J. Lett. **285**, L45 (1984).
[17] A. D. Dolgov *et al.*, Zh. Eskp. Teor. Fiz. **94**, 1 (1988) [Sov. Phys. JETP **67**, 1517 (1988)].
[18] T. J. Broadhurst *et al.*, Nature (London) **343**, 726 (1990).
[19] R. Sancisi and T. S. van Albada, in *Dark Matter in the Universe,* Proceedings of the IAU Symposium, Princeton, New Jersey, 1985, edited by J. Kormendy and G. Knapp, IAU Symposium No. 117 (Reidel, Dordrecht, 1987).
[20] J. R. Bond, in Proceedings of "After the First Three Minutes" Workshop, 1990, edited by C. Bennett, S. Holt, and V. Trimble (unpublished).